



LJMU Research Online

Guo, H, Isserlin, R, Emili, A and Burniston, JG

Exercise-responsive phosphoproteins in the heart.

<http://researchonline.ljmu.ac.uk/id/eprint/7308/>

Article

Citation (please note it is advisable to refer to the publisher's version if you intend to cite from this work)

Guo, H, Isserlin, R, Emili, A and Burniston, JG (2017) Exercise-responsive phosphoproteins in the heart. Journal of Molecular and Cellular Cardiology, 111. pp. 61-68. ISSN 1095-8584

LJMU has developed **LJMU Research Online** for users to access the research output of the University more effectively. Copyright © and Moral Rights for the papers on this site are retained by the individual authors and/or other copyright owners. Users may download and/or print one copy of any article(s) in LJMU Research Online to facilitate their private study or for non-commercial research. You may not engage in further distribution of the material or use it for any profit-making activities or any commercial gain.

The version presented here may differ from the published version or from the version of the record. Please see the repository URL above for details on accessing the published version and note that access may require a subscription.

For more information please contact researchonline@ljmu.ac.uk

<http://researchonline.ljmu.ac.uk/>

Exercise-responsive phosphoproteins in the heart.

Hongbo Guo¹, Ruth Isserlin¹, Andrew Emili^{1*} and Jatin G Burniston^{2†}

¹Donnelly Centre for Cellular & Biomolecular Research, Department of Molecular Genetics, University of Toronto, Ontario, M5S 3E1, Canada. ²Research Institute for Sport & Exercise Sciences, Liverpool John Moores University, Liverpool, L3 3AF, United Kingdom.

*Address for Correspondence: Professor Andrew Emili
Donnelly Centre for Cellular & Biomolecular Research,
University of Toronto,
160 College St,
Toronto ON, M5S 3E1,
Canada.
Tel: +1 416 946 7281
Email: andrew.emili@utoronto.ca

†Address for Correspondence: Professor Jatin G Burniston
Research Institute for Sport & Exercise Sciences
Liverpool John Moores University,
Tom Reilly Building, Byrom Street,
Liverpool, L3 3AF,
United Kingdom.
Tel: +44 151 904 6265
Email: j.burniston@ljmu.ac.uk

29 **Abstract**

30 Endurance exercise improves cardiac performance and affords protection against cardiovascular diseases but
31 the signalling events that mediate these benefits are largely unexplored. Phosphorylation is an widely studied
32 post-translational modification involved in intracellular signalling, and to discover novel phosphorylation
33 events associated with exercise we have profiled the cardiac phosphoproteome response to a standardised
34 exercise test to peak oxygen uptake (VO₂peak).

35 Male Wistar rats (346 ± 18 g) were assigned to 3 independent groups (n= 6, in each) that were familiarised
36 with running on a motorised treadmill within a metabolic chamber. Animals performed a graded exercise test
37 and were killed either immediately (0 h) after or 3 h after terminating the test at a standardised physiological
38 end point (i.e. peak oxygen uptake; VO₂peak). Control rats were killed at a similar time of day to the
39 exercised animals, to minimise possible circadian effects. Cardiac proteins were digested with trypsin and
40 phosphopeptides were enriched by selective binding to titanium dioxide (TiO₂). Phosphopeptides were
41 analysed by liquid chromatography and high-resolution tandem mass spectrometry, and phosphopeptides were
42 quantified by MS1 intensities and identified against the UniProt knowledgebase using MaxQuant (data are
43 available via ProteomeXchange, ID PXD006646).

44 The VO₂peak of rats in the 0 h and 3 h groups was 66 ± 5 ml•kg⁻¹•min⁻¹ and 69.8 ± 5 ml•kg⁻¹•min⁻¹,
45 respectively. Proteome profiling detected 1169 phosphopeptides and one-way ANOVA found 141 significant
46 (P<0.05 with a false discovery rate of 10 %) differences. Almost all (97 %) of the phosphosites that were
47 responsive to exercise are annotated in the PhosphoSitePlus database but, importantly, the majority of these
48 have not previously been associated with the cardiac response to exercise. More than two-thirds of the
49 exercise-responsive phosphosites were different from those identified in previous phosphoproteome profiling
50 of the cardiac response to β₁-adrenergic receptor stimulation. Moreover, we report entirely new
51 phosphorylation sites on 4 cardiac proteins, including S81 of muscle LIM protein, and identified 7 exercise-
52 responsive kinases, including myofibrillar protein kinases such as obscurin, titin and the striated-muscle-
53 specific serine/threonine kinase (SPEG) that may be worthwhile targets for future investigation.

54 **Keywords:**

55 Proteomics; phosphorylation; time-series; cardiac muscle; exercise; maximum oxygen uptake

56

57 **Abbreviations:**

58 Adrenergic receptor (AR), Carbon dioxide production (VCO₂), Electrospray ionisation (ESI), False discovery

59 rate (FDR), High-energy collision-induced dissociation (HCD), Mass spectrometry (MS), Oxygen uptake

60 (VO₂), Peak oxygen uptake (VO_{2peak}), Tandem mass spectrometry (MS/MS), Serine (S), Titanium dioxide

61 (TiO₂), Threonine (T), Tyrosine (Y).

62

63 **1. Introduction**

64 Exercise has an irrefutable role in preventing heart failure and cardiac diseases, for example acute exercise has
65 cardio-protective effects similar to ischaemic preconditioning {Frasier 2011} and chronic exercise training
66 results in physiological cardiac hypertrophy {Bernardo 2016} and a heart phenotype that affords protection
67 against pathological insults such as ischaemia/reperfusion injury {Powers 2008}. Although the physiological
68 benefits of exercise are clear, less is known about the molecular mechanisms that underlie these effects. Yet
69 greater molecular understanding could enable the benefits of exercise to be further optimised or personalised
70 and could suggest new targets for more effective modes of diagnosis, prevention or rehabilitation of
71 debilitating cardiac diseases.

72 Previous work has investigated discrete signalling events activated in response to exercise, for example in the
73 context of acute cardiac preconditioning {Frasier 2011} or adaptive versus maladaptive cardiac
74 hypertrophy {Bernardo 2016}. The IGF-1 receptor/PI3K (p110 α)/ Akt1 pathway is perhaps the most well-
75 explored regulatory pathway associated with exercise-induced cardiac hypertrophy but it is unlikely that a
76 biological phenomenon as complex as cardiac growth is entirely mediated by a single pathway and more often
77 integrated networks of molecules across multiple pathways are required to achieve physiological adaptations
78 to environmental stimuli {Bhalla 1999}. Therefore, events outside of the canonical IGF-1R/ PI3K(p110 α)/
79 Akt1 pathway are likely to also contribute to exercise-induced cardiac adaptations and remain to be
80 discovered.

81 Vigorous exercise is associated with significant elevations in cardiac work and myocardial contractility which
82 are driven by the chronotropic and inotropic effects of beta-adrenergic receptor (AR) signalling (sympathetic
83 drive) as well as local metabolic responses and mechanical strain. In addition to driving acute increases in
84 cardiac output, the molecular events associated with exercise also instigate adaptive processes that alter the
85 cardiac proteome {Burniston 2009} and increase the capacity for work (i.e. VO₂peak). Phosphorylation
86 networks are recognised widely in the literature and are known to transduce signals involved in the skeletal
87 muscle response to exercise in humans {Hoffman 2015} but until now the cardiac phosphoproteome response
88 to exercise has not been reported. Phosphoproteome profiling is a useful approach to discover the pathways
89 and signalling events involved in physiological processes, and a key advantage of this technique is its non-

90 targeted approach that it is not biased by preconceptions about which pathways or events may be of greatest
91 importance.

92 Due to the implausibility of sampling human cardiac tissue in the context of exercise physiology, models are
93 required that simulate exercise prescription in humans while allowing access to the heart for molecular
94 investigation. The exercise stimulus is a composite of 3 inter-related variables, i.e. exercise intensity, duration
95 and frequency, and the cardio-protective of exercise is intensity-dependent {Frasier 2011}. Therefore, to
96 control and standardise exercise intensity we {Burniston 2009} have used indirect calorimetry and an
97 incremental protocol of exercise on a motorised treadmill to measure peak oxygen uptake (VO_{2peak}) of rats
98 in a manner that is equivalent to best practice in human studies (e.g. {Holloway 2009}). During the VO_{2peak}
99 test the animal's respiratory gases are monitored and the test is terminated when the animal reaches its peak
100 aerobic capacity (this intensity of exercise is attainable even by previously sedentary animals). By using this
101 physiological end-point we minimise the influence of acute stress induced by an unrealistic exercise load.
102 Such, standardisation is important because differences in exercise capacity exist even within a colony of
103 animals exposed to identical environmental conditions. Therefore, exposure to the same relative exercise
104 stimulus represents an optimised model with the best chances of successfully identifying the key regulatory
105 networks that mediate exercise-induced adaptation.

106

107 **2. Methods**

108 **2.1. Graded treadmill test of peak oxygen uptake**

109 Experiments were conducted under the British Home Office Animals (Scientific Procedures) Act 1986 and
110 according to UK Home Office guidelines. Male Wistar rats were bred in-house in a conventional colony and
111 the environmental conditions controlled at 20 ± 2 °C, 45-50% humidity with a 12-h light (1800-0600) and
112 dark cycle. Water and food (containing 18.5% protein) were available ad libitum.

113 Exercise sessions were conducted during the animals' dark period. All rats ($n = 18$) completed a 14-day
114 familiarization procedure encompassing daily bouts (15 min duration) at various belt speeds and inclines on a
115 motorized treadmill within a metabolic chamber (Columbus Instruments, OH). On the 15th day the VO_{2peak}
116 of animals ($n = 12$) assigned to the exercise groups was measured using an incremental test, as described
117 previously {Burniston 2009; Burniston 2008}. Briefly, a warm-up (5 min running at $6 \text{ m}\cdot\text{min}^{-1}$, 0° incline)
118 was completed followed a series of 3 min stages of alternating increases in speed (increments of $2 \text{ m}\cdot\text{min}^{-1}$)
119 and incline (increments of 5° ; maximum incline 25°). Air pumped ($2.5 \text{ l}\cdot\text{min}^{-1}$) through the chamber was
120 analysed for concentrations of oxygen and carbon dioxide (Oxymax system; Columbus Instruments, OH;
121 calibrated to an external standard) and a metal grid at the rear of the treadmill belt, which delivered a
122 maximum of 3 electric stimuli (0.1 mA , 0.3 s duration), was used to encourage the animals to achieve their
123 VO_{2peak} . Independent groups ($n = 6$, in each) of animals were killed by cervical dislocation either
124 immediately (0 h) after cessation of the exercise test or 3 h after completing the exercise test. Hearts were
125 isolated from the exercised animals and from control rats ($n = 6$) that completed the familiarization training
126 but did not perform an incremental exercise test. Hearts were rapidly isolated, cleaned and weighed before
127 being stored at -80 °C. To minimize the influence of circadian differences, control rats were killed at a time of
128 day coinciding with the incremental exercise test.

129

130 **2.2. Sample preparation**

131 Left ventricles were pulverized in liquid nitrogen and an accurately weighed portion (100 mg) homogenized
132 on ice in 10 volumes of 8 M urea, 4% w/v CHAPS, 40 mM Tris base including protease and phosphatase
133 inhibitor cocktails (Roche Diagnostics, Lewes, UK) at 4 °C. After centrifugation at $20,000 \text{ g}$, 4 °C for 45 min

134 the supernatant was decanted and the protein concentration measured using a modified 'microtitre plate'
135 version of the Bradford assay (Sigma, Poole, Dorset, UK).

136 Aliquots containing 2 mg protein were reduced with 2.5 mM dithiothreitol for 1 h at room temperature then
137 alkylated with 5 mM iodoacetamide for 45 min in the dark at room temperature. Samples were diluted with 50
138 mM ammonium bicarbonate to bring the concentration of urea to 1M and sequencing-grade trypsin (Promega)
139 was added at a substrate to enzyme ratio of 50:1. After 4 h, samples were diluted threefold with 50 mM
140 ammonium bicarbonate containing additional trypsin, and the digestion was allowed to proceed overnight.
141 After acidification to a final concentration of 1 % (v/v) formic acid, the peptide solutions were desalted using
142 disposable Tiptip C18 columns (Glygen) and lyophilized to dryness. Phosphopeptides were selectively
143 enriched by binding to titanium dioxide (TiO₂)-coated magnetic beads (Pierce) according to the
144 manufacturer's instructions, as described in previously {Guo 2013}. Briefly, peptides were resuspended in
145 200 µL 80 % acetonitrile, 2 % formic acid and incubated for 1 min with 10 µL of slurry containing TiO₂
146 magnetic beads. Unbound peptides and supernatant were decanted and the beads were washed three times
147 with 200 µL binding buffer (supplied with the kit). After final decanting, the beads were incubated for 10 min
148 with 30 µL elution buffer and the eluate was carefully removed and dried prior to mass spectrometry analysis.

149

150 2.3. Mass spectrometry analysis

151 Tryptic peptide mixtures were analysed by nano-scale high-performance liquid chromatography (Proxeon
152 EASY-Nano system) and online nano electrospray ionization (ESI) tandem mass spectrometry (LTQ-Orbitrap
153 Velos mass spectrometer; Thermo Fisher Scientific). Samples were loaded in aqueous 0.1% (v/v) formic acid
154 via a trap column constructed from 25 mm of 75 µm i.d. silica capillary packed with 5 µm Luna C18
155 stationary phase (Phenomenex). The analytical column was constructed in a 100 mm × 75 µm i.d. silica
156 capillary packed with 3 µm Luna C18 stationary phase. Mobile phase A, consisted of 5 % acetonitrile and 0.1
157 % formic acid, and organic phase B contained 95 % acetonitrile and 0.1 % formic acid. Reverse phase
158 separation was performed over 120 min at a flow rate of 300 nL/min, rising to 6 % B in 1 min then from 6 %
159 to 24 % B over 89 min followed by a 16 min gradient to 100 % B, which was held for 5 min prior to re-
160 equilibration to 0 % B over 9 min. Eluted peptides were sprayed directly in to an LTQ-Orbitrap Velos mass

161 spectrometer using a nanospray ion source (Proxeon). Tandem mass spectrometry (MS/MS) was performed
162 using high-energy collision-induced disassociation (HCD) and 10 MS/MS data-dependent scans (7,500
163 resolution) were acquired in centroid mode alongside each profile mode full-scan mass spectra (30,000
164 resolution), as reported previously {Guo 2013}. The automatic gain control (AGC) for MS scans was 1×10^6
165 ions with a maximum fill time of 250 ms. The AGC for MS/MS scans was 3×10^4 , with 150 ms maximum
166 injection time, 0.1 ms activation time, and 40% normalized collision energy. To avoid repeated selection of
167 peptides for MS/MS a dynamic exclusion list was enabled to exclude a maximum of 500 ions over 30 s.

168

169 2.4. Protein identification

170 Data files (RAW format) were searched using the standard workflow of MaxQuant (version 1.3.0.5;
171 <http://maxquant.org/>) against a non-redundant rat protein sequence FASTA file from the UniProt/ SwissProt
172 database modified to contain porcine trypsin sequences. The search parameters allowed 2 missed cleavages,
173 carbamidomethylation of cysteine (fixed) and variable oxidation of methionine, protein N-terminal acetylation
174 and phosphorylation of STY residues. Precursor ion tolerances were 20 ppm for first search and 6 ppm for a
175 second search. The MS/MS peaks were de-isotoped and searched using a 20 ppm mass tolerance. A stringent
176 false discovery rate threshold of 1 % was used to filter candidate peptide, protein, and phosphosite
177 identifications. The mass spectrometry proteomics data have been deposited to the ProteomeXchange
178 Consortium via the PRIDE {Vizcaíno 2016} partner repository with the dataset identifier PXD006646.

179

180 2.5. Bioinformatic Analysis

181 Raw intensities were extracted from the MaxQuant evidence files using an in-house Perl script. Briefly, the
182 intensities from each biological replicate were collapsed to a specific phosphorylation site as opposed to a
183 specific peptide. The residue number (e.g. S224 – phosphorylation on the 224th residue (serine) of the protein)
184 was extracted from the FASTA file used for the original MaxQuant protein search and in any given biological
185 replicate every intensity that can attributed to S224 is summed. If multiple phosphorylations exist on a peptide
186 then the intensities are counted only for the multi-phosphorylation, i.e. single, double and multi
187 phosphorylation become different entities and are scored accordingly. Phospho expression sets were

188 normalized in R using quantile normalization in the limma package. Each modification was scored for
189 differential expression using one-way analysis of variance (ANOVA) across the 3 different time points
190 (control, 0 h and 3 h) complemented by independent t-tests of each pairwise comparison (i.e. 0 h vs control,
191 and 3 h vs control). The false discovery rate (FDR) was assessed by calculating q values {Storey 2003} from
192 the p value distribution of the ANOVA outputs. Protein identifiers associated with statistically significant
193 ($P < 0.05$, FDR $< 10\%$) exercise-responsive phosphopeptides were uploaded to David GO
194 (<https://david.ncifcrf.gov>) {Huang 2009; Huang 2009b} for functional annotation and association to KEGG
195 pathways. Hierarchical clustering was performed using the Graphical Proteomics data Explorer (GProX)
196 {Rigbolt 2011} and protein interactions were investigated using bibliometric mining in the search tool for the
197 retrieval of interacting genes/proteins (STRING; <http://string-db.org/>) {Franceschini 2013}.

198

199 2.6. Western blot analyses

200 Immuno-detection of selected targets was performed using previously described {Burniston 2014} methods.
201 Briefly, samples containing 50 μg protein were resolved by denaturing gel electrophoresis and transferred on
202 to polyvinylidene difluoride membranes. Non-specific protein interactions were blocked by incubating the
203 membranes with 5 % non-fat dry milk in 20 mM Tris, 150 mM NaCl, and 0.1% Tween 20, pH 7.6 (TBS-T)
204 for 1 hr at room temperature. Membranes were then washed in TBS-T and incubated overnight with TBS-T
205 containing 5 % BSA and primary antibodies specific for: p38 mitogen activated protein kinase (p38 MAPK;
206 9212 Cell Signalling Technology; 1:1,000 dilution) and phosphorylated (T180/Y182) p38 MAPK (9211 Cell
207 Signalling Technology; 1:1,000 dilution) or alpha B crystallin (CRYAB; ab13497 Abcam; 1:10,000 dilution)
208 and phosphorylated (S59) CRYAB (ab5577 Abcam; 1:5,000 dilution). Serial washes in TBS-T were per-
209 formed prior to and after incubation with secondary antibodies (goat anti-rabbit IgG; ab205718 Abcam;
210 1:20,000 dilution) in 5 % BSA in TBS-T for 2 h followed by enhanced chemiluminescence (ECL Prime; GE
211 Healthcare) and digitization (Gel Doc XRS; Bio-Rad, Hercules, CA) of immuno-reactive protein bands.
212 Image analysis (Quantity One, version 4.; Bio-Rad) was used to measure the relative abundances of target
213 proteins. Analysis of phosphorylated and non-phosphorylated species was achieved by stripping (incubation

214 in 62.5 mM Tris, 70 mM SDS, 50 mM β -mercaptoethanol, pH 6.8 at 50 °C for 30 min) and re-probing of
215 membranes.

216

217 **3. Results**

218 Three independent groups (n= 6, in each) of rats were used to investigate the time course of changes in the
219 heart phosphoproteome in response to a standardised bout of endurance exercise. The body weight or heart
220 weight of rats assigned to the control, 0 h and 3 h groups was similar and rats that performed the incremental
221 exercise test (i.e. 0 h and 3 h groups) had equivalent peak exercise capacities (Table 1). An example of VO₂
222 VCO₂ traces recorded during an incremental exercise test is illustrated in Figure 1. The average time to
223 complete the incremental exercise test was 21 min and the average VO_{2peak} of animals in the 0 h and 3 h
224 groups was $66 \pm 5 \text{ ml}\cdot\text{kg}^{-1}\cdot\text{min}^{-1}$ and $69.8 \pm 5 \text{ ml}\cdot\text{kg}^{-1}\cdot\text{min}^{-1}$, respectively.

225 LC-MS/MS profiled 1,169 phosphopeptides and there were 841 singly phosphorylated peptides were detected
226 and of these 11 were pY, 90 were pT and 840 were pS. There were also 289 doubly phosphorylated peptides,
227 30 triply phosphorylated and 10 peptides that had between 4 and 6 phosphorylated residues. One-way
228 ANOVA found 141 peptide differences at $P < 0.05$, the false discovery rate (FDR) calculated from q values
229 {Storey 2003} was estimated to be 10 %. Volcano plots are illustrated in Figure 2 to highlight post-hoc
230 analysis of phosphopeptides that differed between the control and 0 h group (Figure 2A) or between control
231 and 3 h group (Figure 2B). Immediately after cessation of exercise similar numbers of phosphopeptides were
232 increased and decreased in abundance compared to control. After 3 h recovery (Figure 2B) the majority of
233 phosphopeptides were more abundant in exercised hearts compared to control.

234 The 141 peptides that significantly differed in response to acute exercise mapped to 97 proteins, i.e. some
235 proteins had more than one phosphopeptide. Examples of proteins that had multiple phosphorylated peptides
236 include titin (10 peptides), tensin (5 peptides), Bcl2-interacting death suppressor (5 peptides), alpha-2-HS-
237 glycoprotein (4 peptides), pyruvate dehydrogenase E1 component subunit alpha (4 peptides) and isoform 2 of
238 NDRG2 protein (3 peptides).

239 Exercise-responsive phosphopeptides were uploaded to David GO for functional annotation and the top
240 ranking significant ($P < 0.05$; Fischer with BH correction) KEGG pathways were arrhythmogenic right
241 ventricular cardiomyopathy, cardiac muscle contraction and adrenergic signalling in cardiomyocytes.

242 Mapping to PhosphoSitePlus (<http://www.phosphosite.org>) found all but 4 (97 %) of the identified
243 phosphopeptides had previously been reported. The most commonly reported phosphosites matching to
244 published high-throughput (MS2) data were pyruvate dehydrogenase E1 component subunit alpha
245 S232&S239, gap junction alpha-1 protein S325& S328, septin-2 S218 and heat shock protein beta-1 S15.
246 Approximately 28 % (39 of 141) of the exercise-responsive phosphorylation sites were also associated with
247 low-throughput experimental evidence in PhosphoSitePlus, including p38 mitogen-activated protein kinase
248 Y182, cardiac phospholamban S16, alpha B-crystallin S59 and cardiac troponin I S23. Western blot analysis of
249 phosphorylated and non-phosphorylated forms of p38 MAPK and alpha B crystallin (Figure 3) verified
250 statistically significant differences in the phosphorylation status of these proteins discovered by LC-MS/MS
251 phosphopeptide profiling.

252 The time-series experimental design was used to provide further associational evidence between
253 phosphorylation events and the cardiac exercise response. Hierarchical cluster analysis was performed in
254 GProX to find similarities in the temporal patterns of exercise responsive phosphopeptides (n = 141, P<0.05).
255 The temporal responses in phosphopeptide abundance organised in to 3 prominent clusters (Figure 4A). Gene
256 identifiers of exercise responsive phosphoproteins from each cluster were uploaded to STRING and Panels B,
257 C and D of Figure 4 illustrate interaction networks within each cluster based on literature and database
258 information, including co-expression, protein-protein interaction and literature mining.

259

260 **4. Discussion**

261 The mediators of exercise-induced cardiac adaptation have been less thoroughly investigated than the
262 mechanisms of pathological cardiac maladaptation, but greater knowledge regarding the physiological
263 responses of the heart could provide a valuable contrast to data from pathological models. To address this
264 need, we performed phosphoproteomic profiling to generate new knowledge regarding the cardiac
265 phosphoproteome response to exercise. To minimise potential mis-identification of phosphorylation events
266 that may be associated with a supra-physiological cardiac stress rather than the response to physiological
267 exercise, the oxygen uptake (Figure 1) of each animal was monitored and the exercise test was terminated at a
268 standardised physiological end point (VO₂peak). We discovered entirely new phosphorylation sites on 4
269 cardiac proteins (Table 2), including S81 of muscle LIM protein, and identified 7 exercise-responsive kinases
270 (Table 3). Almost all (97 %) of the phosphosites that responded significantly to exercise (supplementary Table
271 S1) were annotated in the PhosphoSitePlus database but, importantly, the majority of these had not previously
272 been associated with the cardiac response to exercise. Therefore the current data provides a rich source of new
273 information relating to the potential mediators of exercise-induced cardiac protection.

274 Muscle LIM protein (MLP; also known as cysteine and glycine-rich protein 3) is an essential component of
275 myogenic differentiation {Arber 1994} and contains 2 LIM domains which facilitate protein-protein
276 interactions. LIM domain containing proteins are important mediators of signals between the cytoskeleton and
277 nucleus {Kadmas 2004} and we discovered a new phosphorylation of S81 (significantly greater 3 h after
278 exercise) which lies within a flexible region between LIM domain 1 (residues 10-61) and LIM domain 2
279 (residues 120-171) of MLP and is close to a previously reported site (S95) that is phosphorylated during beta-
280 1 AR stimulation {Lundby 2013}. Other phosphorylation sites of rat MLP include S111 and S153 but
281 phosphorylation/ de-phosphorylation of these sites has not yet been linked to environmental stimuli or cell
282 signalling processes. MLP can interact with a number of myogenic factors {Kong 1997} and also proteins at
283 the myofibril z-disc, including alpha-actinin {Geier 2003}, beta-spectrin {Flick 2000} and the titin capping
284 protein, telethonin/ TCAP {Knöll 2002}. Translocation of MLP from the sarcomere to the nucleus is
285 facilitated by a nuclear localisation signal (residues 64-69) and inhibition of MLP nuclear translocation
286 prevents the protein synthetic response to cyclic strain in cardiomyocytes {Boateng 2009}.

287 We speculate MLP may also be involved in transducing signals in response to exercise in vivo and the novel
288 S81 phosphorylation reported here may influence the protein-protein interactions and subcellular localisation
289 of MLP. The amino acid sequence flanking S81 of MLP (Table 1) does not match the linear motifs recognised
290 by well-defined protein kinases, but our phosphoproteome profiling identified a selection of exercise-
291 responsive myofibrillar protein kinases (Tables 2 and 3) that could be potential mediators of MLP S81
292 phosphorylation at the z-disc. Two novel exercise-induced phosphorylation events (Table 2) were discovered
293 on myofibrillar protein kinases (myosin light chain kinase 3 and obscurin) and may be involved in the
294 transduction of mechanical signals within the exercised heart. Myosin light chain kinase 3 is responsible for
295 the phosphorylation of ventricular regulatory myosin light chain, which contributes to the enhancement of
296 myocardial contractility {Kampourakis 2016} and we report novel S444 phosphorylation of myosin light
297 chain kinase 3 occurs during vigorous exercise (Cluster 1).

298 Obscurin is also a member of the myosin light chain kinase family along with striated muscle-specific
299 serine/threonine kinase (SPEG; Table 3) and these kinases are predicted to target similar conserved sites
300 {Sutter 2004} and may be involved in the hypertrophic response of the heart {Borisov 2006}. In exercised
301 hearts, we discovered greater phosphorylation of obscurin S2974, which has not previously been reported, and
302 phosphorylation of SPEG S2410 & S2414 that was reported {Lundby 2013} in phosphoproteome profiling of
303 the cardiac response to β 1-adrenergic receptor (AR) stimulation. Phosphorylation of SPEG has also recently
304 been reported {Potts 2017} in phosphoproteome analysis of mouse skeletal muscle submitted to a bout of
305 maximal isometric contractions. These independent discoveries of SPEG phosphorylation using non-targeted
306 techniques provide reciprocal verification and further highlight SPEG as an exercise-responsive
307 phosphoprotein/ kinase of interest for future mechanistic study. Phosphorylation of the giant myofibrillar
308 protein kinase, titin, was also detected after exercise (Table 3) and each of the titin phosphorylation sites
309 reported here (Table S1) is also known to be responsive to β 1-AR stimulation. Taken together, our data
310 describe a collection of myofibrillar protein kinases and phosphorylation events associated with the z-disc
311 region that are responsive exercise and warrant further investigation as mediators of exercise-induced cardiac
312 adaptation.

313 Exercise training has protective effects against cardiomyocyte death and proteins that interact with Bcl-2
314 family members involved in the regulation of apoptosis and autophagy were enriched amongst the exercise-
315 responsive phosphoproteome. We discovered new phosphorylation sites (T93 and Y94; Table 1) on Bcl-2
316 interacting killer-like protein (Bik) which became significantly more phosphorylated 3 h after cessation of
317 exercise. These sites are different to the previously reported ERK1/2 mediated phosphorylation of Bik at
318 T124 that is associated with ubiquitination and subsequent degradation of Bik {Lopez 2012} and represent
319 new targets for further exploration. Phosphorylation of BCL2/adenovirus E1B 19 kDa-interacting protein 3
320 (BNIP3) was increased after exercise and this protein has been implicated in the regulation of both apoptosis
321 and mitophagy {Choe 2015} in a manner similar to the better characterised protein Beclin-1 {Maejima 2016}.
322 In addition, exercise was associated with phosphorylation of Bcl-2-interacting death suppressor (Bag3) on
323 sites (S176, S277, S278, S377, S387) previously reported in response to beta-adrenergic receptor stimulation
324 {Lundby 2013}. Bag3 is a co-chaperone of heat shock cognate 70 (hsc70), interacts with heat shock protein
325 22 and regulates the interaction with poly-glutamate (Poly-Q) proteins which are prone to aggregation.
326 Phosphorylation of S397 of Bcl-2 associated transcription factor 1 (BCLAF1) increased after cessation of the
327 exercise (cluster 3) and this protein is required for efficient DNA repair and genome stability {Savage 2014}.
328 Together our findings describe an unappreciated network of responses in proteins that regulate apoptosis and
329 autophagy processes, beyond the more widely reported effector proteins such as Bcl-2 and Bax.

330 During exercise myocardial contractility increases to meet the greater demand for cardiac output and this
331 response is in part driven by β -AR signalling. Approximately one-third (41 of 141 phosphopeptides) of the
332 exercise-responsive phosphopeptides were previously identified in similar phosphoproteome profiling
333 {Lundby 2013} of the cardiac response to β_1 -AR stimulation, including PKA and archetypal proteins involved
334 in myocardial contractility/ Ca^{2+} -handling and metabolism. For example, ryanodine receptor phosphorylation
335 increased during exercise (Figure 4, Cluster 1) and this has previously been associated with augmentation of
336 intracellular calcium release and enhanced myocardial contractility {Marx 2000}. The SERCA inhibitor,
337 phospholamban, was phosphorylated at S16, which is noted to be sufficient for a maximal cardiac response to
338 β -AR stimulation {Chu 2000}, and in addition, we report phosphorylation of lesser-known proteins such as
339 histidine-rich calcium binding protein that also regulates SR calcium release {Arvanitis 2011}. With regard to

340 metabolism, exercise increased S694 phosphorylation of phosphorylase kinase beta (Table 3) which is
341 responsible for phosphorylation of glycogen phosphorylase and therefore acceleration of glycogenolysis. The
342 monocarboxylate transporter 1 (Slc161a) was also phosphorylated at a β_1 -AR responsive site immediately
343 after exercise and this may be associated the transport lactate or ketones in to cardiac muscle cells.
344 Conversely, phosphorylation of the pyruvate dehydrogenase E1 complex subunit alpha (Pdha1) is associated
345 with inhibition of pyruvate entry to the TCA cycle and was increased 3 h after the cessation of exercise
346 (Figure 4, Cluster 3) and may be more associated with restoration of cardiac glycogen stores. Notably,
347 phosphorylation sites reported here in response to exercise and by Lundby et al {Lundby 2013} in response to
348 β_1 -AR stimulation do not entirely overlap, and even after taking in to account potential technical differences
349 between the 2 studies, it is evident that the cardiac exercise response is not entirely driven by β_1 -AR
350 stimulation.

351 Cardiac β_1 -AR stimulation is associated with the activation of p38 MAP kinase {Lundby 2013} and this was
352 also detected in response to exercise (Table 3 and Figure 3A). Previous {Hunter 2008} targeted (western blot)
353 analysis of signalling proteins in hearts of high- and low-capacity runner rats isolated 10 min after performing
354 a ramped treadmill test measured a 1.6-fold increase in p38 MAPK (T180/Y182) phosphorylation, which is
355 corroborated by our data (Figure 3A). We further show Y182-specific phosphorylation of p38 MAPK
356 (measured by LC-MS; Table S1) is transient and was not significantly different from control 3 h after
357 exercise. Moreover the change in p38 MAPK phosphorylation clusters with the phosphorylation of proteins
358 including alpha B-crystallin, heat shock protein 27 and astrocytic phosphoprotein PEA-15 (Figure 4; Cluster
359 1). Astrocytic phosphoprotein PEA-15 modulates the localisation and activity of ERK 1/2 MAP Kinases
360 (MAPK1 and MAPK3), phosphorylation of PEA-15 at both S104 and S106 is necessary and sufficient to
361 prevent its interaction with ERK 1/2 whereas non-phosphorylated PEA-15 blocks the nuclear translocation
362 and transcriptional capacity of ERK 1/2 {Krueger 2005}. In the current work PEA-15 was phosphorylated at
363 S104 only, but nonetheless the exercise-responsive phosphoproteome was enriched for proteins involved in
364 ERK1/2 mitogen-activated protein kinases pathway and approximately 18 % (25 of 141) of the cardiac
365 phosphorylation sites reported here have previously been identified as ERK1/2 targets by phosphoproteomic
366 analysis of epithelia cells {Courcelles 2013}.

367 MEK1-ERK1/2 signalling can inhibit Calcineurin-NFAT signalling which is strongly implicated in
368 pathological cardiac hypertrophy {Molkentin 2004}. Given the large degree of cross-talk between these
369 pathways more intricate studies are needed to decipher the networks of interactions associated with
370 pathological versus physiological cardiac adaptations, and the role of currently lesser known components such
371 as Cyma5 costamere protein, which was phosphorylated in response to exercise, and is a negative regulator of
372 calcineurin-NFAT signalling cascade {Molkentin 2004} will need to be integrated with the existing canonical
373 pathways.

374 The IGF-1 receptor/PI3K (p110 α)/ Akt1 pathway is the most thoroughly studied signalling pathway
375 associated with exercise-induced cardiac adaptation and is associated with Akt S473 phosphorylation {Weeks
376 2012}. We found no significant change in Akt S473 phosphorylation after an acute bout of treadmill running
377 which is consistent with previous {Hunter 2008} findings and suggests a single exercise bout is not sufficient
378 to instigate the IGF-1 receptor signalling in the heart. Nonetheless, acute exercise was associated with
379 phosphorylation of direct regulators of ribosomal translation such as eukaryotic initiation factors eIF2 and
380 eIF5. The interaction between eIF-5B and eIF2 β is essential for GTP hydrolysis and release of eIF2-GDP
381 from the 40 S initiation complex and the formation of the 80 S ribosome. Phosphorylation of eIF2 clustered
382 with ATP-binding cassette sub-family F member 1 (ABCF1) and this interaction (including S109
383 phosphorylation of ABCF1) has previously been reported to be necessary in both cap-dependent and
384 independent translation {Paytubi 2009}. Therefore our findings draw attention to regulators of ribosomal
385 translation initiation that have largely been ignored in previous exercise-related studies.

386 A single bout of exercise can precondition the heart against I/R damage {Frasier 2011} and gap junction
387 proteins could be a key mechanism underlying this protective effect {Jeyaraman 2012}. Gap junction alpha-1
388 protein (Cx43) is the main component of gap junctions in the ventricular myocardium and phosphorylation of
389 S325, S328 and T326 of Cx43 increased 3 h after exercise. Cx43 has a short (<5 h) half-life and
390 phosphorylation is required for gap junction formation whereas de-phosphorylation is associated with the
391 disassembly of the gap junction and Cx43 degradation {Solan 2007}. Phosphorylation at 325, 328 and 330
392 reported here may be mediated by casein kinase 1 {Cooper 2002} or fibroblast growth factor {Sakurai 2013}
393 and regulate gap junction assembly {Lampe 2006}. In contrast, Cx43 S262 phosphorylation has more

394 commonly been associated with cardiac preconditioning mediated via PKC {Waza 2014} and was not
395 responsive to exercise. Therefore the current findings highlight a novel exercise-induced mechanism
396 involving gap-junction assembly/ turnover separate from those involved in ischaemic preconditioning. In
397 addition, phosphorylation of CX43 co-occurred with the phosphorylation of tight junction protein 2,
398 Palkophillin-2 and the alpha subunit of the voltage-gated sodium channel (Figure 4, Cluster 3), which have
399 previously been reported as interaction partners.

400

401 **5. Summary**

402 Signal transduction is a dynamic process and we used a time-series design to dissect immediate/early events
403 such as phospholamban phosphorylation (Figure 4; Cluster 1), which may be more associated with myocardial
404 contractility, from sustained (Figure 4; Cluster 2) or latter (Figure 4; Cluster 3) phosphorylation events that
405 may be more associated with the adaptive response to exercise or the restoration of cardiac homeostasis. Non-
406 targeted analysis detected well established phosphorylation events associated with myocardial contractility
407 whilst simultaneously detecting new site-specific phosphorylation events on proteins that are not shared with
408 the cardiac response to β_1 -AR stimulation and have not previously been associated with the cardiac exercise
409 response. In particular, we discovered new phosphorylation sites on 4 cardiac proteins (Table 2), including
410 S81 of muscle LIM protein, and identified a selection of myofibrillar protein kinases that were also responsive
411 to exercise and may constitute a putative network of signal transduction for the adaptation to mechanical work
412 in the heart.

413

414 **Disclosures**

415 None

416 **Funding**

417 This work was supported by Liverpool John Moores University.

418

419 **References**

420 {Bibliography}

421

422 **Table 1 – Physical and physiological characteristics**

	Control	0 h	3 h
Body weight (g)	338 ± 16	350 ± 27	351 ± 9
Heart weight (mg)	1071 ± 44	1005 ± 76	1060 ± 40
VO ₂ peak (ml•kg ⁻¹ •min ⁻¹)		66 ± 5	69.8 ± 5
Peak RER		1.046 ± 0.03	1.021 ± 0.03
Time to completion (min)		21.3 ± 3.6	21.3 ± 3.1

423 Data are presented as Mean ± SD (n = 6, in each group). There were no statistically significant (p<0.05) differences between the groups for any
 424 of the variables measured.

425

426

427

428

429 **Table 2 – New site-specific phosphorylation sites discovered in cardiac proteins**

Cluster	Protein name	UniProt	Residue	(+/-)7 Sequence
1	Myosin light chain kinase 3	E9PT87	S444	TEAGRRVSpSAAEAAI
2	Obscurin	A0A0G2K8N1	S2974	LGLTSKASpLKDSGEY
3	Cysteine and glycine-rich protein 3	P50463	S81	GQGAGCLSpTDTGEHL
3	Bcl2-interacting killer-like protein	Q925D2	T93 & Y94	MHRLAATpYpSQTGVR

430

431

432

433

Table 3 – Phosphorylated kinase enzymes

Cluster	Protein name	UniProt	Residue
1	Myosin light chain kinase 3	E9PT87	S444
1	p38 mitogen-activated protein kinase	Q56A33	Y182
1	Phosphorylase kinase beta	Q5RKH5	S694
1	Titin	Q9JHQ1	S402
1	Titin	Q9JHQ1	S1990
2	cAMP-dependent protein kinase	P09456	S77 & S83
2	Obscurin	A0A0G2K8N1	S2974
2	Striated muscle specific serine/threonine kinase	Q63638	S2410 & S2414
2	Titin	Q9JHQ1	S256 & T267
2	Titin	Q9JHQ1	S32863
3	cAMP-dependent protein kinase	P09456	S83
3	Titin	Q9JHQ1	T300 & S302
3	Titin	Q9JHQ1	S1332 & S1336

435

436

437

438

439

440 **Figure Legends**

441 **Figure 1 - Measurement of VO₂peak**

442 Example oxygen uptake (VO₂) and carbon dioxide production (VCO₂) traces during an incremental
443 exercise test designed to elicit peak oxygen uptake (VO₂peak).

444

445 **Figure 2 - Changes in the abundance of exercise responsive phosphopeptides**

446 Volcano plots presenting the distribution of the fold-change (log₂) in abundance and statistical
447 significance of phosphorylated peptides. Post-hoc comparisons are shown for (A) non-exercised
448 control hearts vs hearts isolated immediately (0 h) after cessation of the graded exercise test, or (B)
449 non-exercised control hearts vs hearts isolated 3 h after cessation of the graded exercise test.

450

451 **Figure 3 – Exercise responsive phosphorylation of cardiac p38 MAPK and CRYAB**

452 Western blot analysis of the ratio of phosphorylated: non-phosphorylated p38 mitogen activated
453 kinase (p38 MAPK; A) and alpha B crystallin (CRYAB; B). Cropped images of 3 representative lanes
454 from a single animal from the control, 0 h and 3 h groups are shown. Data are presented as mean ±
455 SEM (*n* = 6, per group) and statistical significance (**P*<0.05 different from control group) was
456 determined by one-way analysis of variance and Tukey HSD post-hoc analysis.

457

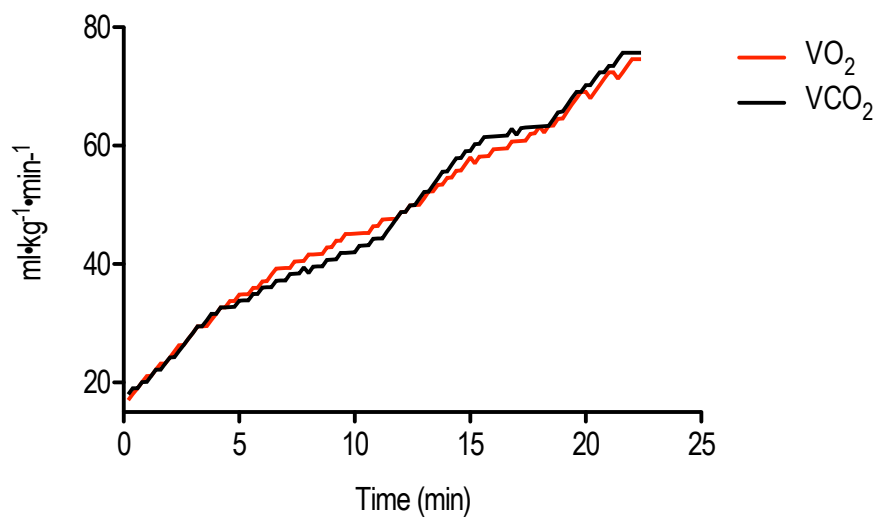
458 **Figure 4 – Hierarchical clustering of exercise responsive phosphopeptides**

459 Unsupervised hierarchical clustering was performed on 141 phosphopeptides that exhibited statistically
460 significant (*P*<0.05) differences across time by one-way ANAVO. Known and predicted interactions
461 between proteins within each cluster were then investigated using the Search Tool for the Retrieval of
462 Interacting Genes/Proteins (STRING). (A) **Cluster 1** contains phosphopeptides whose abundance
463 significantly increased immediately after exercise and then returned to basal levels within 3 h after
464 cessation of the exercise test; this cluster included phosphorylation of phospholamban (Pln) and a
465 network of p38α (MAPK14) stress-responsive proteins including alpha B-crystallin (Cryab) and heat

466 shock 27 kDa protein (Hspb1). (B) **Cluster 2** contains phosphopeptides whose abundance increased
467 immediately after exercise and further increased 3 h after cessation of the exercise test; this cluster
468 included phosphorylation of costamere and gap junction proteins such as vincullin and connexin 43
469 (Gja1). In addition, ribosomal proteins, such as eukaryotic initiation factor 2 (eIF2s2) and ATP
470 binding cassette sub-family F member 1 (Abcf1), which regulate both cap-dependent and independent
471 translation were phosphorylated in response to exercise. (C) **Cluster 3** contains phosphopeptides
472 whose abundance decreased immediately after exercise and then returned to basal levels within 3 h
473 after cessation of the exercise test; this cluster included phosphorylation of myofibrillar proteins,
474 including muscle LIM protein (Csrp3).

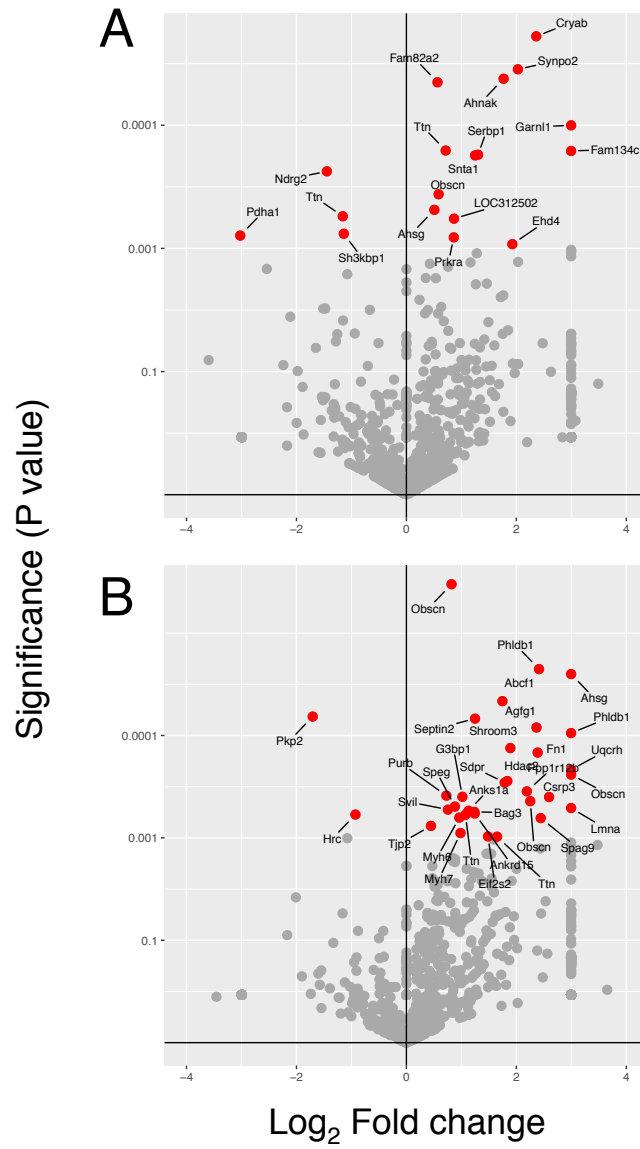
475

476 **Figure 1**

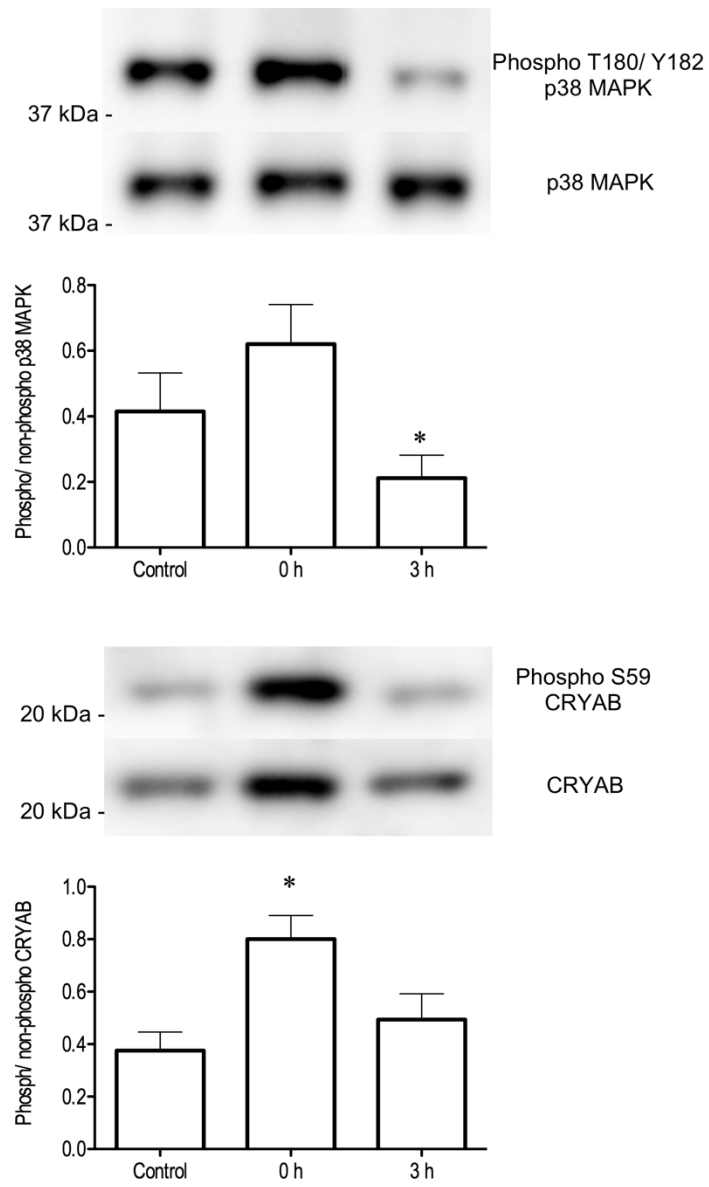


477

478

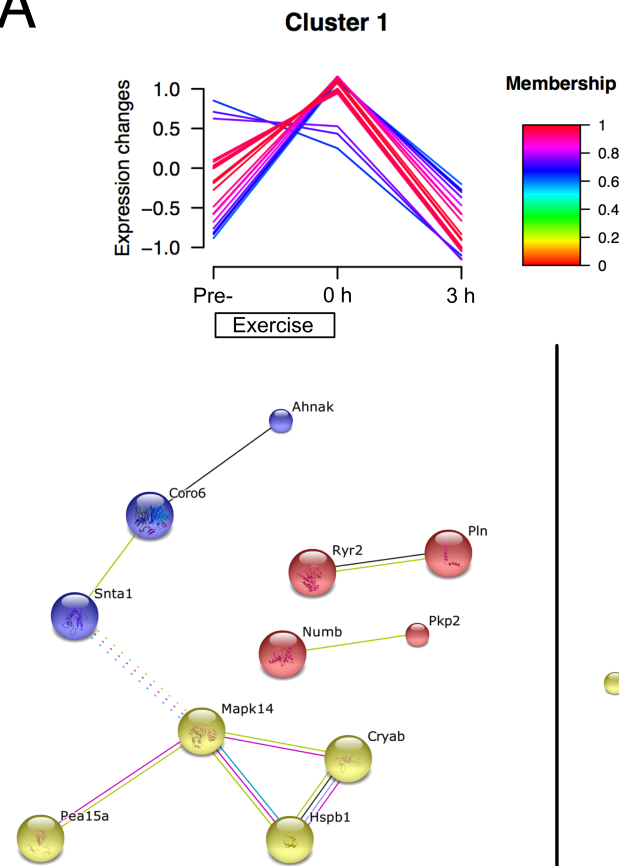


483 **Figure 3**

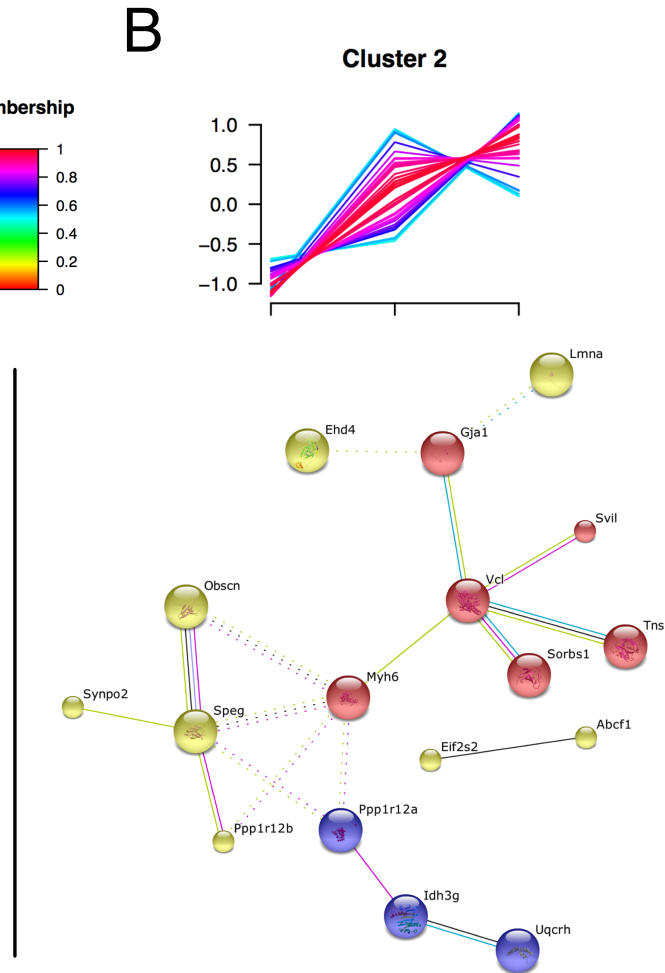


484
485

A



B



C

